Evaluation of Nanospray Capillary LC-MS Performance for Metabolomic Analysis in Complex Biological Matrices

Authors

Mahmoud Elhusseiny Mostafa[1], James P. Grinias[2], James L. Edwards[1*]

Affiliations

1 Department of Chemistry and Biochemistry, Saint Louis University, 3501 Laclede Ave, St Louis, MO 63102, USA

2 Department of Chemistry & Biochemistry, Rowan University, 201 Mullica Hill Rd., Glassboro, NJ 08028, USA

Corresponding Author:

*James L. Edwards:
3501 Laclede Ave, St Louis, MO 63102, USA
jim.edwards@slu.edu

Abstract

LC-MS metabolomic analysis in complex biological matrices may be complicated by degeneracy when using large-bore columns. Degeneracy is the detection of multiple mass spectral peaks from the same analyte due to adduction of salts to the metabolite, dimerization, or loss of neutrals. This introduces interferences to the MS spectra, diminishes quantification, and increases the rate of false identifications. Analysis using 2.1 mm inner diameter (i.d.) columns typically leads to degenerate peaks whereas nanospray using capillary columns (25, 50, and 75 µm i.d.) reduces degeneracy. Optimization of chromatographic parameters of capillary LC for amino acid standards showed the lowest HETP at 1.25 mm/sec across all capillary i.d. columns. Results suggest mass-sensitive detection below the optimum velocity. At faster velocities, concentration-dependent detection occurred across all capillaries.

The 2.1 mm i.d. analytical scale column showed the greatest level of degeneracy, particularly in the low signal intensity range. 25 µm i.d. columns showed higher levels of metabolite annotation for the same signal intensity range. It also provided the lowest level of degeneracy, making it best suited for untargeted analysis. The 25 µm i.d. column achieved a peak capacity (n_c) of 144 in a 30-minute gradient method with n_c decreasing as the column i.d. increased. 75 µm i.d. capillary columns showed the highest signal intensity, which is beneficial for targeted analysis. These effects of chromatographic performance, resolution, and degeneracy profile of capillary and analytical scale columns were compared for metabolomic analyses in complex serum and cell lysate matrices.

Keywords:

Metabolomics, optimization, capillary LC, nanospray, HPLC, MS, ion trap, orbitrap, degeneracy, human serum, *E. coli*

1. Introduction

The analysis of small molecules in complex biological samples is important to understanding disease phenotypes, unraveling biochemical pathways, and uncovering potential biomarkers. LC-MS is currently the dominant platform for large-scale metabolomic analysis due to its high sensitivity, selectivity, and throughput. Metabolomic data from LC-MS platforms are often complicated by degeneracy, which is the observation of multiple interfering peaks arising from a single analyte during the electrospray process.[1] These interferents come from inefficiencies of the electrospray process and include adduction of salts to the analyte, dimerization, or loss of neutrals such as H_2O or NH_3. Such interfering peaks can lead to false identifications. Other experimental factors that play a role in degeneracy include velocity, volumetric flow rate, and spray tip diameter.

Capillary LC-MS (capLC-MS) with nano-ESI has generated substantial benefits in proteomics with regards to analyte detection and quantification, particularly in sample limited cases. Nanospray produces smaller droplets than full ESI, which improves ionization efficiency, sensitivity, and potentially reduces degeneracy.[2] CapLC-MS in proteomics has increased peptide coverage by 50%, leading to the identification of thousands of proteins in a single cell.[3] Improved sensitivity, resolution, peak capacity, and peptide identification for small sample volumes have been observed for shotgun proteomic analysis[4] when using capLC-MS over larger bore columns. Multidimensional capLC-MS has also been shown to result in a greater number of proteins and peptides identified on a wider dynamic range in cell lysates compared to analytical scale 2D-SCX-RP separation.[5] These proteomic studies demonstrate that improvements in capillary column performance inherently improve MS detection in complex samples. While capLC-MS has become mainstream in proteomics, its transition to metabolomics is limited.

Metabolomic analysis using analytical scale columns is limited by poor signal-to-noise, long analysis time, and high-pressure requirements.[6] CapLC-MS typically provides higher sensitivity and metabolomic coverage than a full-bore.[7] CapLC-MS analysis has been undertaken in a limited capacity for metabolomic and lipidomic analyses.[8, 9] Peak capacity (n_c) of 150 in a 30min. run had been achieved using a 20cm 2.1mm full-bore column.[10] Recently, n_c of 350 in 60 min. were achieved using 20cm 100 μm i.d. columns for the analysis of human plasma samples by optimizing particle size, column length, gradient time, injection volume, and pressure. This led to an improved resolution which increased the peak capacity and hence the number of the features detected.[9] Improvements in peak detection can be seen by further decreasing the diameter, as 53,986 features were detected in the untargeted analysis of diabetic murine aortas when using a 50 μm i.d. column. This resulted in the identification of 48 altered metabolic pathways.[11] Metabolomic profiling of human urine and human sweat using nanoflow capLC-MS combined with chemical isotope labeling provided better sensitivity and wider dynamic range compared to microbore-LC, improving quantification accuracy.[12]

CapLC has shown substantial benefits to chromatographic performance,[13] overall detector responses,[14] and improvements in sensitivity.[15] Despite these improvements,

capLC investigations into the effect of column i.d. and detector performance in high sensitivity metabolomics have yet to be evaluated.[16] This work examines the effects of capillary column i.d. on chromatographic parameters and MS detection in the complex biological matrices of bacterial cell lysate and human serum.

2. Materials and Methods

2.1. Reagents and columns.

25, 50, and 75 μm i.d. (360 μm outer diameter) fused silica capillary were purchased from Polymicro Technologies (Phoenix, AZ USA). A Zero dead volume (ZDV) IDEX High-Pressure PEEK union was purchased from Cole-Parmer (Vernon Hills, IL). The analytical-scale column was an Atlantis 2.1 x 150 mm column packed with 3 μm C18 particles from Waters (Milford, MA USA). The same packing material was obtained for use in preparing capLC columns. LCMS grade water, acetonitrile, formic acid, and hydrofluoric acid, as well as analytical grade trimethylolpropane trimethacrylate, glycidyl methacrylate, benzoin methyl ether, toluene, and isooctane, were all purchased from Fisher Scientific (Pittsburgh, PA USA). Amino acids standards (serine, proline, tyrosine, phenylalanine, tryptophan) were from Acros Organics (Fair Lawn, NJ USA). Human serum NIST 909c was purchased from the National Institute of Standards and Technology (Gaithersburg, MD USA) and an isotopic internal standard of algal amino acids mixture (^{13}C algal, >97%) was purchased from Cambridge Isotope Laboratories Inc. (Tewksbury, MA USA).

2.2. Sample preparation.

2.2.1. Amino Acids Standard Mixture.

Serine, proline, tyrosine, phenylalanine, and tryptophan were each dissolved in water to create 8 mM standard stock solutions in separate vials. From these stock solutions, a mixture containing 25 μM was prepared in 75/25 H_2O/acetonitrile with 0.1% formic acid. Standard solutions were kept at -20°C until use.

2.2.2 Human Serum Sample.

100 μL of human serum NIST 909c standard was added to a solution made of 1 mg of ^{13}C algalmix dissolved in 4 mL of 80/20 methanol/H_2O. The mixture was centrifuged at *21,100xg* at a temperature of 2°C for 5 minutes. The supernatant was collected and dried. The sample was then reconstituted in 200 μL of H_2O and stored at -80°C until use.

2.2.3. *E. coli* Lysate Sample.

40 mg/μL of *E. coli* lysate extract was dried in room temperature under a vacuum centrifuge, then reconstituted in 200 μL of H_2O and stored at -80°C until use.

2.3. Chromatography.

2.3.1. Packing capillary column.

Capillary columns with nano tip orifices were fabricated using a trap-end frit, laser-pulled method.[17] Briefly, windows were generated in a 30 cm long fused silica capillary using an

electrical arc to remove the polyimide coating. Photopolymerized frits were generated using a monomer mix of 350 µL trimethylolpropane trimethacrylate and 150 µL of glycidyl methacrylate with 7.9 mg of benzoin methyl ether. The porogenic solvent was prepared by mixing 250 µL toluene and 750 µL isooctane. The monomer solution (300 µL) was added to the porogen solution and sonicated for 15 minutes. The frit mixture was loaded into the capillary column and polymerization was initiated under a UV lamp (UVP, Cambridge, UK). The reaction took 30 minutes at ambient temperature with an exposure wavelength of 365 nm at 6 W (0.12 A). Nanospray tips were generated using a laser fiber puller model P-2000 (Sutter Instruments, Novato, CA, USA) with heating time: 420 msec, velocity: 80 msec, delay time: 150 msec, pulling time: 225 msec. The nano emitter fritted capillary was etched in hydrofluoric acid (51%) to open the fine tip for nanospray capLC-MS. Capillary columns with different i.d.s (25, 50, and 75 µm) were packed in-house with T3 Atlantis 3-micron particles using a gas pressure cell.[2, 17] Final capillary column lengths were trimmed to 15 cm.

2.3.2. Isocratic Method.

The Agilent LC pump (Agilent Infinity 1260 LC pump system) connected to LTQ XL Linear Ion Trap and was set to flow a mobile phase of 75/25 H_2O/acetonitrile (with 0.1% formic acid). To achieve nanoflow on the ESI spraying tip, velocities were split at ratios described in **Table 1**: The standards mixture was analyzed at different velocities ranging from 0.5 to 4.0 mm/sec. For normalization of performance variation between different columns of the same i.d., three packed columns of each i.d. and triplicate trials of each volumetric velocity were performed. Reported efficiency values are based on an average of n = 9 runs, excluding the outliers identified by a Grubbs test.

2.3.3. Gradient Method.

The Thermo Scientific LC pump (Thermo Fisher Vanquish quaternary pump model-F) connected to a Q-Exactive Orbitrap Mass Spectrometer with flow solvent A: H_2O (+0.1% formic acid) and solvent B: acetonitrile (+0.1% formic acid). The gradient for LC solvent was as follows (minute, %B): 0 min, 0%; 5 min, 0%; 25 min, 98%; 28 min, 98%;29 to 48 min, 0%.

2.4. Injection.

2.4.1. On-column injection.

Capillary columns were inserted inside a pressure cell containing the sample at 100 psi for 13 sec to load the sample to ~1% of the total capillary column volume. The column was then mounted to the outlet of the flow splitter tee for analysis. For mass versus concentration sensitive detection experiments, the loading time was increased to 26 sec and 65 sec to increase the injected volume two-fold and five-fold, respectively.

2.4.2. Autosampler injection.

The Thermo Scientific autosampler injection was used with the Vanquish UHPLC system and 0.1mm/0.004” according to the manufacturer guidelines. It was used for the 2.1mm

analytical scale full-bore column injections. For capLC analysis of the human serum and E. *coli* samples, it was done using the split-flow ratios described in **Table 1.** The LC pump was used to achieve the velocity and the volumetric flow rates in the nanoflow range. This system loads the sample to ~1% of the total capillary column volume. QE Orbitrap MS autosampler temperature was set at 5°C during analysis.

2.4.3. Autosampler injection.

Investigation into extra column band broadening was performed by direct injection of the five amino acids standards individually into the Vanquish HPLC system. This was done using the same tubing in section 2.4.2 and replacing the column with a ZDV connection.

2.5. Detector: Mass Spectrometer.

2.5.1. Linear Ion Trap.

Column optimization experiments were performed on an LTQ XL Linear Ion Trap mass spectrometer (Thermo Fisher Scientific, San Jose, CA) at 2.0 kV spray voltage in positive ionization mode. The mass range was from 50-250 m/z, maximum injection time 10 msec, the capillary temperature of 200°C, and capillary voltage of 9 V.

2.5.2 High-Resolution Q-Exactive Orbitrap.

Complex sample analysis was performed on a Q-Exactive Orbitrap mass spectrometer (Thermo Fisher Scientific, Waltham, MA USA) for detection and fragmentation analysis of metabolites in human serum and *E. coli* lysate samples at a 2.0 kV spray voltage in positive ionization mode. The capillary temperature was 200°C. Collision-induced dissociation was performed in the HCD cell with a normalized collision energy of 35.0% and an isolation window of 0.4 u. Spectra were collected at a mass range of 70-900 m/z with a mass resolution of 140,000 (R_{FWHM}) and automatic gain control (AGC) of 1E6.

The Q-Exactive Orbitrap mass spectrometer performed fragmentation experiments with the following settings: the resolution was set to 35,000, AGC target of 5E5, maximum injection time was 50 msec, loop count of 5, isolation window of 0.4 m/z, normalized collision energy N(CE) of 35%, and dynamic exclusion was 10 sec.

2.6. DATA PROCESSING

2.6.1. Peak Fit.

For initial column characterization, data files in (.RAW) format were displayed on Thermo Xcalibur Qual browser software from Thermo Scientific and chromatogram data points were exported to PeakFit software (Systat Software Inc., San Jose, CA, USA). Peaks were fitted to the linear fit baseline model (3%) with Savitsky-Golay smoothing of 1%. Chromatographic Gaussian peak mode was used for peak identification, with R^2 values representing how close the data fit to perfect gaussian shape ranging between 0.82 – 0.97.

2.6.2. Wilke-Chang Equation.

For calculation of reduced velocity, diffusion coefficients of amino acids in solution were calculated using the Wilke-Chang Equation.[18, 19] The estimated diffusion coefficients are based on the theoretical partial molal volume (mL/mol), mobile phase association factor[20], temperature, and solvent viscosity.

2.6.3. MS-Dial.

Verification of the selected analytes was performed by data-dependent scan using the Q-Exactive Orbitrap mass spectrometer and MSDial software. In complex sample analysis, untargeted LC-MS data were analyzed using MS Dial. Data files in (.RAW) format were converted to (.mtd2). These data files then were uploaded to MS-Dial 4.24 RIKEN® and processed with a mass tolerance range (0.01 – 0.025), minimum mass peak height (5E4), and mass slice width (0.05 Da). The selected database for matching features was "All public MS/MS (13,303 unique compounds)" in positive mode with 290,915 features (unique compounds plus degeneracy). Non-matched fragments of the sample and the database were filtered out and the matched fragmentations were displayed.

2.6.4. XCMS, METLIN, and HMDB.

Human serum and *E. coli* lysate samples were analyzed with gradient split-flow capillary LC-Q-Exactive Orbitrap mass spectrometer. Data were analyzed by XCMS [21, 22] with prefilter intensity of 1000, a maximum peak width of 60 sec, and a minimum peak width of 10 sec. Features were considered significant with the following criteria: p-value ≤ 0.05, fold change ≥ 1.5, intensity ≥ 5000, retention time between 2 and 25 min. The resulting data were used to check the total number of features and the total number of $[M+H]^+$ features found in the XCMS database, METLIN,[23] and human metabolome database HMDB.[24]

2.6.5. CAMERA, metID and VennDiagram.

CAMERA is a Bioconductor package of R packages software (RStudio, Boston, MA) that provides interfaces for integrating algorithms to extract identified features, spectra, annotate isotope, adduct peaks, and propose the accurate compound mass against the Manchester Metabolome Database (MMD) in a highly complex data frame.[25] The algorithm uses HMDB and METLIN databases. For features detection, XCMS centWave algorithm was used with the following parameters: snthresh = 5, ppm = 10, peakwidth = (5,20), prefilter = (2,200). Feature alignment was performed with the standard *group.density* algorithm from XCMS with bw = 3 and mzwid = 0.015. For the display of degenerate features map, each minute in the MS scan was binned as a bar in the histogram.

Common annotated features across the analytical scale and capillary columns were identified using metID[26] and VennDiagram packages (downloadable from R-studio software). The algorithm uses HMDB and KEGG database. The analysis was done using the following parameters: 10 ppm, retention time tolerance = 10 sec, retention time match weight = 0.25, thread number = 5, total score tolerance 0.5.

2.6.6. SEM imaging.

To determine the nanospray orifice size, scanning electron microscope (SEM) imaging was done on the laser-cut HF-etched capillaries. They were sputter-coated with gold metal at 30 mA for 40s using a vacuum chamber (Denton Vacuum LLC, NJ USA). The sputter-coated capillaries were imaged by an SSD camera Inspect F50 model. The SEM (FEI, Hillsboro, OR) was operated at 10 kV acceleration voltage to give the optimum image pixels. The tip size images were analyzed using the ImageJ software (National Institutes of Health, Bethesda, MD USA).[27] SEM was used to image three capillary columns of each i.d. and average the tip diameter as shown in the **(Supplemental Table 1)** to normalize for variation of tip morphology across different columns of the same i.d.

3. Results and discussion.

3.1. Capillary Column Characterization/Evaluation

The overall goal of this study was to determine the most suitable chromatographic conditions for metabolomic analysis of complex samples using capLC-MS. To achieve this, the capillary column performance was evaluated in 25, 50, and 75 μm i.d. columns with five amino acids as standard analytes. **Figure 1A** shows changes in HETP as a function of velocity for serine and tryptophan. Consistent with previous work,[2] 25 μm i.d. columns resulted in superior chromatographic performance, particularly in optimum velocity ranges (0.85-1.50 mm/sec) for serine. When examining five amino acids, all capillaries showed roughly the same optimum velocity of 1.25 mm/sec The analytical scale 2.1 mm column showed optimum velocity was between 1–2mm/sec. It showed relatively higher HETP and a less steep increase in *H* at higher velocities **(Supplemental Figure S-1)**. This may be attributed to extra-column band broadening.[28-30] Direct infusion of the five amino acids standards individually on the Vanquish-UHPLC without the column showed the band broadening due to the connection tubing and ESI apparatus **(Supplemental Figure S-3)**. The extra column effects account for approximately 2-fold reduction in plate number and therefore a 2-fold increase in plate height. The capillary columns have an embedded emitter tip which dramatically minimizes the post-column variance. Increasing the velocity resulted in less band broadeningfound in both ZDV experiments and using the 2.1mm full-bore column.

Diffusion coefficient (D_m) values were 1.79, 1.48, 1.12, 1.14 and 1.02 x10^{-5} cm^2/sec for 75:25 water:ACN for serine, proline, tyrosine, phenylalanine and tryptophan respectively. These were used to plot the *h* versus reduced velocity (*v*) plots **(Supplemental Figure S-2)**. After normalizing for particle size, similar results were observed when examining reduced plate heights, which ranged from *h* = 1.6 to *h* = 3.6 for 25 μm i.d. columns. The superior performance of the 25 μm i.d. column was expected as using 3 μm particles in a 25 μm i.d. capillary column gives a column-to-particle diameter ratio of 8.3. Ratios below 10 yield better performance due to more homogeneous packing from the wall region occupying the majority of the cross-section.[13]

Signal intensity in a nanospray capLC-MS system can be characterized as either mass-sensitive or concentration-sensitive depending on the velocity, ionization efficiency, and the nature of the analyte.[31] The shift from mass sensitive to concentration sensitive detection over increasing velocity indicates a difference in nanospray efficiency. At low velocities, the nanospray is highly efficient and thus changes in overall mass will lead to

proportional changes to signal response. At higher velocities, this efficiency inherently decreases and the ability to ionize these analytes diminishes as mass increases, likely due to competing ionization. All three capillaries showed similar trends along with increasing velocities despite having substantially different volumetric flow rates. This strongly suggests that within the capillary regime, the velocity is substantially more important to the electrospray efficiency than is the volumetric flow rate for the analytes investigated.

Results suggest velocities slower than 1.00 mm/sec exhibit mass-sensitive detection in our system. Faster velocities shift the electrospray MS response from mass to concentration-sensitive detection. This observation is not ubiquitous for all amino acid standards. The transition from mass to concentration-sensitive detection was mostly observed in the polar analyte serine. The transition was less pronounced with increasing hydrophobicity shown in proline, tyrosine, phenylalanine to tryptophan **(Supplemental Figure S-4)**. The same percentage (1%) of the capillary column volumes were loaded for all capillary i.d.s. The i.d. of the capillary column, therefore, dictates the mass injected at the same velocity as shown in **Table1**. The mass injected from the 75µm i.d. capillary was around 9 times more than from the 25µm i.d. whereas 50µm i.d. capillary was 4 times greater than the 25µm i.d. Smaller capillary column diameter generally showed decreasing signal intensity. This is attributed to the smaller sample amount injected into the detector.

Examination of the early eluting analyte, serine, showed negligible signal intensity change from 25 µm to 50 µm i.d. The transition was more pronounced from 50 µm to 75 µm i.d. Increasing the hydrophobicity gave a better distinction of the mass to concentration transition across all the i.d.s used in our system. This suggests that the differences in detector intensity may be attributed to a combination of velocity and analyte hydrophobicity and that the shift between mass and concentration-sensitive detection is not always distinct.[32, 33] The signal response at the optimum velocity of 1.25 mm/sec, hydrophobic compounds showed lower LOD for the 75 µm i.d. capillary. This could be attributed to the charge residual model in electrospray ionization.[34] More hydrophobic analytes are more likely to escape the charged ESI droplet. The rapid ejection from the droplet may boost the signal intensity and the MS detection sensitivity.[34] Lower LOD (fmol range) and higher sensitivity were found for 25 µm i.d. for all analytes.

Examination of the nanospray tip of each column showed that the 25 and 50 µm i.d. had emitter tip diameters of ~500 nm, whereas the 75 µm i.d. columns had four-fold larger tips of 2 µm. Despite multiple attempts, the 75 µm i.d. capillary tips could not be reduced to a 500 nm size using our laser-pulling method. To evaluate the spray tip and column diameter on analyte signal, the same mass was injected onto all three capillaries (Supplemental Figre S-5A). These data show that signal intensities were superior for the smaller i.d. than the larger i.d. capilleries when performed in the mass sensitive regime. In general, capLC showed a good signal response compared to the 2.1mm column. The nano-sized emitter tip results in higher ionization efficiency and sensitivity. This is of course beneficial for sample limited cases.

The overall evaluation of the mass vs. concentration response suggests that MS detector response is dependent largely on the velocity and the analyte hydrophobicity. Based on these data, the volumetric flow rate did not indicate a shift in the MS detection

from mass to concentration sensitivity. The spray efficiency was found to control MS signal intensity in a mass-sensitive detection regime **(Supplemental Figure 5)**. Chromatographic optimization is essential for maintaining sensitivity in a complex matrices that contain analytes of different hydrophobicities. Optimization of the capillary system allows for investigations into chromatographic resolution, signal response, and degeneracy in complex samples.

3.2. Complex Biological Sample Analysis

After the capillary performance and detector response were characterized, complex samples were investigated using high-resolution MS to evaluate the effects of velocity on chromatographic resolution. Metabolite extracts from human serum were analyzed at three different velocities (0.65; 1.25; and 1.75 mm/sec) with varying column diameters **(Figure 2 A-C)** using a pressurized chamber injection scheme. These velocities were chosen to represent slow, optimum, and fast velocities, where slow and fast rates are expected to yield nearly equivalent plate height. Sphingosine (SP) and dihydrospingosine (HSP) were chosen as model analytes to evaluate chromatographic resolution due to their close elution proximity **(Supplemental Figure S-6 A, B)**. As capillary i.d. decreased, resolution tended to increase at each of the three velocities. As expected, the estimated optimum velocity yielded the highest resolution.

As pressurized chamber injections are time-consuming and labor-intensive, sample introduction via an autosampler before the flow split was also evaluated. The resolution from standard autosampler injections onto an analytical scale 2.1 mm i.d. column was compared to split-based injections onto 25, 50, and 75 µm i.d. capillary columns under varying velocities **(Figure 2D-G)**. The analytical scale column showed HETP values nearly double that of the capillary columns **(Supplemental S-1 and S-2)**. At very high velocity (4mm/sec), HETP values of capLC and the full-bore columns were very close. This may be attributed to the mass transfer contribution to band broadening being more significant in the capillary system.[35] This explains the lower resolution at the velocities tested. The change in the HETP trend of the analytical scale column was substantially less steep than the capillary columns. This provided close HETP values across 1 to 2 mm/sec, which resulted in comparable resolution between 1.25 and 1.75 mm/sec compared to the loss of resolution in capillary columns that had steeper HETP increases at higher velocities.

Comparison of these data to the pressurized chamber injection of the same type of capillary columns suggests that the autosampler inherently provides more band broadening.[36] This is explained by the longer pathway the sample plug experiences as it travels from the autosampler to the analytical column. Pressurized chamber injections load the sample directly onto the column which eliminates such extra column band broadening effect. At 25 µm i.d., velocities of 1.25 mm/sec showed optimum performance in HETP and resolution for both on-column direct injection and autosampler injections. The 50 and 75 µm i.d. capillary columns followed the same trend as the direct on-column injection with optimum velocities yielding optimum resolution. Of note is that the resolution from the autosampler split-flow injection was consistently lower than that of the on-column direct injection.

Evaluation of separation performance of capillary and analytical scale full-bore columns was done using peak capacity n_c.[37, 38] Peaks analysis was done on the serum complex biological matrix using gradient elution and autoinjector. The average peak width at 4σ (*i.e.,* width at 13.4% peak height) of maximum signal intensity was done by PeakFit software. The early, middle, and late eluting analytes peak width across the gradient ramp time is in **Supplemental Table 2**. The peak capacity was found to be $n_{c\ 25\ i.d.}$ = 144, $n_{c\ 50\ i.d.}$ = 131, $n_{c\ 75\ i.d.}$ = 116, $n_{c\ 2100\ i.d.}$ = 101 for a 30 min gradient. The smaller the i.d. of the columns resulted in higher the peak capacity. These values could be further enhanced by reducing gradient steepness and extending analysis time although exceptionally long runs do lead to diminishing improvements in peak capacity.

The signal intensities of the five amino acids in human serum and *E. coli* samples were compared across varying column diameters **(Figure 3)**. The 75 µm i.d. had the highest signal intensity in most instances when compared to the analytical scale column (2.1 mm i.d.), 25 µm, and 50 µm i.d. capillaries. The more complex matrix of serum showed less discernable trends with regards to either the mass/concentration sensitive detection or signal response trends with regards to hydrophobicity. The *E. coli* lysate, generally considered a less complex matrix, showed increased signal intensity with increasing column diameter. CapLC analysis of the five amino acids maintained comparable sensitivity in the complex biological matrix. They gave the same signal intensity range as the analytical scale column for all the capillary i.d.s tested.

Injection of a fixed mass of the human serum was analyzed on the capillary columns at 1.25 mm/sec (optimum) velocity. The 25µm i.d. capillary showed higher signal intensity and signal to noise ratio than the 50 µm compared to the 75 µm i.d **(Supplemental Figure S-5 B, C)**. This indicates that for a fixed mass the spraying efficiency controls MS signal more than the mass injected.[13, 34] Taken together, Figure 3 and supplemental Figure 5 show that at a fixed mass injected, smaller i.d. columns showed higher signal, but that for injections of the same capillary volume percentage, the larger capillaries showed higher signal intensity due to more mass injected.

3.3. Degeneracy study.

The degeneracy profile of adducts from the five amino acids in complex matrices **(Figure 4A-E)** was analyzed by XCMS, CAMERA, and verified using METLIN and HMDB database. Results showed considerably more degenerate peaks in the analytical scale columns than in capillary columns. Amongst the capillary columns, degeneracy decreased with column i.d. No degenerate peaks were detected for the five amino acids in the 25 µm i.d. Degenerate peaks often confound quantitation and complicate data analysis in untargeted metabolomics experiments. The decrease in degenerate peaks is likely due to increased spray efficiency derived from the smaller emitter tips and velocities. Degeneracy, as indicated by the proline potassium adducts, was compared in the analytical scale and capillary columns **(Figure 4F)**. **Supplemental Figure S-7** shows an increase in the signal of the degenerate peak as the column i.d. increases.

The total number of features and the identified non-degenerate molecular ions found in human serum and *E. coli* samples **(Figure 5)** were determined by XCMS and CAMERA packages. More features were identified (*i.e.*, annotated) and fewer degenerate peaks were found in the capillary-scale columns. The total number of features in serum was highest for the 2.1 mm i.d. column by a wide margin compared to the capillary

columns. However, evaluation of these peaks indicates that the vast majority (73%) are degenerate, and therefore interferents, as the signal from their corresponding analyte is diminished by their presence **(Figure 3)**. After filtering the data for only annotated metabolites, all columns gave fairly close results within 5% (3234 ± 165). The highest number of both annotated features and non-degenerate but unannotated features come from the 25 μm i.d. columns. Smaller column i.d.s showed a higher number of non-degenerate, un-annotated peaks in serum. This suggests that smaller columns may provide more beneficial data for untargeted metabolomic analyses. Analysis of the *E. coli* samples yielded similar general trends with a lower degeneracy profile. Importantly, the sample complexity of *E. coli* was substantially lower than that of serum as noted by the total number of peaks detected. This difference inherently reduces the amount of degeneracy and is most notable in the 2.1 mm i.d. column. This suggests that matrix effects are most pronounced in the analytical scale column compared to capillary columns. MetID was used to cross-reference the feature identification data analyzed by XCMS online and CAMERA package. A Venn diagram of mutual annotated features across different ESI sources is shown in **Supplemental Figure 8**.

Degenerate signals are often observed at a lower signal intensity range than the parent analyte. The distribution of all analyte and degenerate features across different i.d.s from the serum samples were plotted and analyzed by CAMERA **(Figure 6 A-D)**. The boxed region shows signal intensity lower than 1E5, which can consist of either non-degenerate or degenerate peaks. The volume loaded on the 2.1mm i.d. was 1000-fold higher than the 25μm i.d. capillary. The higher mass injection did not result in improved detection capability. In fact, the lower ionization efficiency of the full-bore column merely generated more degenerate peaks. Comparison of the low intensity regions in the 25 μm and the 2.1 mm i.d. columns show that annotated features generally yield fewer degenerate peaks in the low intensity region for the 25 mm **(Figure 6 E-H)**. The selected features were verified by MSDial analysis of the data-dependent scan **(Figure S-5 C, F)**. The E. *coli* samples followed the same signal intensity distribution trend **(Supplemental Figure 9)**. Taken as a histogram, the total number of degenerate peaks was plotted as a function of elution time **(Supplemental Figure S-10)**. The low intensity features in the capillary system are non-degenerate peaks, whereas the features from the analytical scale column in the same region are from degenerate peaks. This inherently shows that higher spray efficiency in capillary columns yields a higher likelihood of detecting non-degenerate peaks and potentially uncovering novel metabolites. This indicates that for discovery-based metabolomic investigations, the capillary system outperforms the 2.1mm column.

4. Conclusion

Capillary LC columns showed higher sensitivity, peak capacity, resolution, and lower degeneracy than an analytical scale column. Decreasing the capillary i.d. showed fewer degenerate peaks and a higher percentage of annotated features. In addition, injection of the same mass on-column showed higher signal intensity for the smaller capillary indicating the importance of increasing ionization efficiency. The practicality of using the analytical scale column came at the cost of increased degeneracy which decreases the maximum signal of the M+H peak, diminishes the detection limits, distorts the MS data reliability, and deters quantification. Capillary columns for metabolomic

analyses provide the benefits of higher spraying efficiency and lower degeneracy without sacrificing sensitivity.

Untargeted metabolomics for detection and annotation of features has been performed using capLC-MS.[1, 39] These features may be a defined metabolite, unannotated metabolite, or a degenerate with a matching mass with another metabolite. Untargeted analyses matching the database may be biased with the false hits arising from those combinations. This would be more predominant in analytical scale columns where most degenerate features were found. The lower degeneracy of capLC-MS would decrease the chance of these false hits. This makes capLC-MS a better option for uncovering biological pathways and potentially discovering new metabolites. Low signal intensity features analyzed by the 25 µm i.d. column were found to correspond more to identified metabolites from the databases. The 25 µm i.d. column showed the best resolution at the suggested optimized chromatographic conditions. It showed the lowest number of degenerate features which could be related to better ionization efficiency by the smaller ESI droplet. The high peak capacity, better resolution, and lower degeneracy of the 25 µm i.d. column hold the most benefit for untargeted analysis.

Quantitation of targeted metabolomics in complex sample matrices is dependent on the ESI ionization efficiency, signal intensity, and sample complexity.[40] The 75 µm i.d. column showed the highest signal intensity, likely due to higher mass injected. This would benefit targeted analysis, especially for low abundance metabolites in limited biological samples. In general, the capillary columns provided higher sensitivity than the analytical scale 2.1 mm i.d. full bore column for targeted analysis. Variations in nanospray tip geometry were not fully explored in this study, though potentially important to the resulting data sets.

The overall capLC performance suggests more confidence in annotated peaks and quantification than the analytical scale columns for the analysis of complex biological samples. This makes capLC a useful analytical tool for both targeted and untargeted analyses for quantification, determination of biological pathways, and the discovery of new metabolites.

Acknowledgments

This work was supported by funding from the Chemical Measurement and Imaging Program in the National Science Foundation Division of Chemistry to J.L.E. (CHE-1904919), and to J.P.G. (CHE-1904454).

References

1. Sindelar, M.; Patti, G. J., Chemical Discovery in the Era of Metabolomics. *J Am Chem Soc* **2020,** *142* (20), 9097-9105.
2. Edwards, J. L.; Edwards, R. L.; Reid, K. R.; Kennedy, R. T., Effect of decreasing column inner diameter and use of off-line two-dimensional chromatography on metabolite detection in complex mixtures. *Journal of Chromatography A* **2007,** *1172* (2), 127-134.
3. Cong, Y.; Liang, Y.; Motamedchaboki, K.; Huguet, R.; Truong, T.; Zhao, R.; Shen, Y.; Lopez-Ferrer, D.; Zhu, Y.; Kelly, R. T., Improved Single-Cell Proteome Coverage Using Narrow-Bore Packed NanoLC Columns and Ultrasensitive Mass Spectrometry. *Analytical Chemistry* **2020,** *92* (3), 2665-2671.
4. Shishkova, E.; Hebert, A. S.; Westphall, M. S.; Coon, J. J., Ultra-High Pressure (>30,000 psi) Packing of Capillary Columns Enhancing Depth of Shotgun Proteomic Analyses. *Analytical chemistry* **2018,** *90* (19), 11503-11508.
5. Zhou, F.; Cardoza, J. D.; Ficarro, S. B.; Adelmant, G. O.; Lazaro, J.-B.; Marto, J. A., Online Nanoflow RP−RP-MS Reveals Dynamics of Multicomponent Ku Complex in Response to DNA Damage. *Journal of Proteome Research* **2010,** *9* (12), 6242-6255.
6. Broeckhoven, K.; Desmet, G., Advances and Challenges in Extremely High-Pressure Liquid Chromatography in Current and Future Analytical Scale Column Formats. *Analytical Chemistry* **2020,** *92* (1), 554-560.
7. Chetwynd, A. J.; David, A., A review of nanoscale LC-ESI for metabolomics and its potential to enhance the metabolome coverage. *Talanta* **2018,** *182*, 380-390.
8. Sorensen, M. J.; Miller, K. E.; Jorgenson, J. W.; Kennedy, R. T., Ultrahigh-Performance capillary liquid chromatography-mass spectrometry at 35 kpsi for separation of lipids. *Journal of Chromatography A* **2020,** *1611*, 460575.
9. Sorensen, M. J.; Kennedy, R. T., Capillary ultrahigh-pressure liquid chromatography-mass spectrometry for fast and high resolution metabolomics separations. *Journal of Chromatography A* **2021,** *1635*, 461706.
10. Soliven, A.; Haidar Ahmad, I. A.; Filgueira, M. R.; Carr, P. W., Optimization of gradient reversed phase chromatographic peak capacity for low molecular weight solutes. *Journal of Chromatography A* **2013,** *1273*, 57-65.
11. Filla, L. A.; Yuan, W.; Feldman, E. L.; Li, S.; Edwards, J. L., Global metabolomic and isobaric tagging capillary liquid chromatography-tandem mass spectrometry approaches for uncovering pathway dysfunction in diabetic mouse aorta. *Journal of proteome research* **2014,** *13* (12), 6121-6134.
12. Li, Z.; Tatlay, J.; Li, L., Nanoflow LC–MS for High-Performance Chemical Isotope Labeling Quantitative Metabolomics. *Analytical Chemistry* **2015,** *87* (22), 11468-11474.
13. Kennedy, R. T.; Jorgenson, J. W., Preparation and evaluation of packed capillary liquid chromatography columns with inner diameters from 20 to 50 micrometers. *Analytical Chemistry* **1989,** *61* (10), 1128-1135.
14. Zhang, J.; Liu, Y.; Jaquins-Gerstl, A.; Shu, Z.; Michael, A. C.; Weber, S. G., Optimization for speed and sensitivity in capillary high performance liquid chromatography. The importance of column diameter in online monitoring of serotonin by microdialysis. *J Chromatogr A* **2012,** *1251*, 54-62.
15. Schmidt, A.; Karas, M.; Dülcks, T., Effect of different solution flow rates on analyte ion signals in nano-ESI MS, or: when does ESI turn into nano-ESI? *Journal of the American Society for Mass Spectrometry* **2003,** *14* (5), 492-500.
16. Miller, K. E.; Jorgenson, J. W., Comparison of microcapillary column length and inner diameter investigated with gradient analysis of lipids by ultrahigh-pressure liquid chromatography-mass spectrometry. *Journal of Separation Science* **2020,** *43* (22), 4094-4102.

17. Haskins, W. E.; Wang, Z.; Watson, C. J.; Rostand, R. R.; Witowski, S. R.; Powell, D. H.; Kennedy, R. T., Capillary LC−MS2 at the Attomole Level for Monitoring and Discovering Endogenous Peptides in Microdialysis Samples Collected in Vivo. *Analytical Chemistry* **2001,** *73* (21), 5005-5014.
18. Wilke, C. R.; Chang, P., Correlation of diffusion coefficients in dilute solutions. *Aiche Journal* **1955,** *1* (2), 264-270.
19. Li, J.; Carr, P. W., Accuracy of Empirical Correlations for Estimating Diffusion Coefficients in Aqueous Organic Mixtures. *Analytical Chemistry* **1997,** *69* (13), 2530-2536.
20. Zamyatnin, A. A., Protein volume in solution. *Progress in Biophysics and Molecular Biology* **1972,** *24*, 107-123.
21. Forsberg, E. M.; Huan, T.; Rinehart, D.; Benton, H. P.; Warth, B.; Hilmers, B.; Siuzdak, G., Data processing, multi-omic pathway mapping, and metabolite activity analysis using XCMS Online. *Nat Protoc* **2018,** *13* (4), 633-651.
22. Mahieu, N. G.; Genenbacher, J. L.; Patti, G. J., A roadmap for the XCMS family of software solutions in metabolomics. *Current Opinion in Chemical Biology* **2016,** *30*, 87-93.
23. Smith, C. A.; Maille, G. O.; Want, E. J.; Qin, C.; Trauger, S. A.; Brandon, T. R.; Custodio, D. E.; Abagyan, R.; Siuzdak, G., METLIN: A Metabolite Mass Spectral Database. *Therapeutic Drug Monitoring* **2005,** *27* (6).
24. Wishart, D. S.; Tzur, D.; Knox, C.; Eisner, R.; Guo, A. C.; Young, N.; Cheng, D.; Jewell, K.; Arndt, D.; Sawhney, S.; Fung, C.; Nikolai, L.; Lewis, M.; Coutouly, M.-A.; Forsythe, I.; Tang, P.; Shrivastava, S.; Jeroncic, K.; Stothard, P.; Amegbey, G.; Block, D.; Hau, D. D.; Wagner, J.; Miniaci, J.; Clements, M.; Gebremedhin, M.; Guo, N.; Zhang, Y.; Duggan, G. E.; MacInnis, G. D.; Weljie, A. M.; Dowlatabadi, R.; Bamforth, F.; Clive, D.; Greiner, R.; Li, L.; Marrie, T.; Sykes, B. D.; Vogel, H. J.; Querengesser, L., HMDB: the Human Metabolome Database. *Nucleic Acids Research* **2007,** *35* (suppl_1), D521-D526.
25. Kuhl, C.; Tautenhahn, R.; Böttcher, C.; Larson, T. R.; Neumann, S., CAMERA: An Integrated Strategy for Compound Spectra Extraction and Annotation of Liquid Chromatography/Mass Spectrometry Data Sets. *Analytical Chemistry* **2012,** *84* (1), 283-289.
26. Shen, X.; Wu, S.; Liang, L.; Chen, S.; Contrepois, K.; Zhu, Z.-J.; Snyder, M., metID: an R package for automatable compound annotation for LC−MS-based data. *Bioinformatics* **2021**.
27. Schneider, C. A.; Rasband, W. S.; Eliceiri, K. W., NIH Image to ImageJ: 25 years of image analysis. *Nat Methods* **2012,** *9* (7), 671-675.
28. Moussa, A.; Deridder, S.; Broeckhoven, K.; Desmet, G., Detailed computational fluid dynamics study of the parameters contributing to the viscous heating band broadening in liquid chromatography at pressures up to 2500 bar in 2.1 mm columns. *Journal of Chromatography A* **2022,** *1661*, 462683.
29. Spaggiari, D.; Fekete, S.; Eugster, P. J.; Veuthey, J.-L.; Geiser, L.; Rudaz, S.; Guillarme, D., Contribution of various types of liquid chromatography–mass spectrometry instruments to band broadening in fast analysis. *Journal of Chromatography A* **2013,** *1310*, 45-55.
30. Fekete, S.; Fekete, J., The impact of extra-column band broadening on the chromatographic efficiency of 5cm long narrow-bore very efficient columns. *Journal of Chromatography A* **2011,** *1218* (31), 5286-5291.
31. Urban, P. L., Clarifying Misconceptions about Mass and Concentration Sensitivity. *Journal of Chemical Education* **2016,** *93* (6), 984-987.
32. Henriksen, T.; Juhler, R. K.; Svensmark, B.; Cech, N. B., The relative influences of acidity and polarity on responsiveness of small organic molecules to analysis with negative ion electrospray ionization mass spectrometry (ESI-MS). *Journal of the American Society for Mass Spectrometry* **2005,** *16* (4), 446-455.
33. Cech, N. B.; Enke, C. G., Practical implications of some recent studies in electrospray ionization fundamentals. *Mass Spectrometry Reviews* **2001,** *20* (6), 362-387.

34. Konermann, L.; Ahadi, E.; Rodriguez, A. D.; Vahidi, S., Unraveling the Mechanism of Electrospray Ionization. *Analytical Chemistry* **2013,** *85* (1), 2-9.
35. Gritti, F.; Guiochon, G., Mass transfer kinetics, band broadening and column efficiency. *Journal of Chromatography A* **2012,** *1221*, 2-40.
36. Gunnarson, C.; Lauer, T.; Willenbring, H.; Larson, E.; Dittmann, M.; Broeckhoven, K.; Stoll, D. R., Implications of dispersion in connecting capillaries for separation systems involving post-column flow splitting. *Journal of Chromatography A* **2021,** *1639*, 461893.
37. Wang, X.; Stoll, D. R.; Schellinger, A. P.; Carr, P. W., Peak Capacity Optimization of Peptide Separations in Reversed-Phase Gradient Elution Chromatography: Fixed Column Format. *Analytical Chemistry* **2006,** *78* (10), 3406-3416.
38. Hsieh, E. J.; Bereman, M. S.; Durand, S.; Valaskovic, G. A.; MacCoss, M. J., Effects of column and gradient lengths on peak capacity and peptide identification in nanoflow LC-MS/MS of complex proteomic samples. *Journal of the American Society for Mass Spectrometry* **2013,** *24* (1), 148-153.
39. Mahieu, N. G.; Patti, G. J., Systems-Level Annotation of a Metabolomics Data Set Reduces 25 000 Features to Fewer than 1000 Unique Metabolites. *Analytical Chemistry* **2017,** *89* (19), 10397-10406.
40. Yuan, W.; Edwards, J. L., Capillary separations in metabolomics. *Bioanalysis* **2010,** *2* (5), 953-963.

Figure1 – Characterization of capillary column LC-MS.
A) The change in HETP **B)** change in signal intensity as a function of velocity (U) (mm/sec) for serine (left-side) and tryptophan (right-side) using 25, 50, and 75µm i.d. capillary columns.

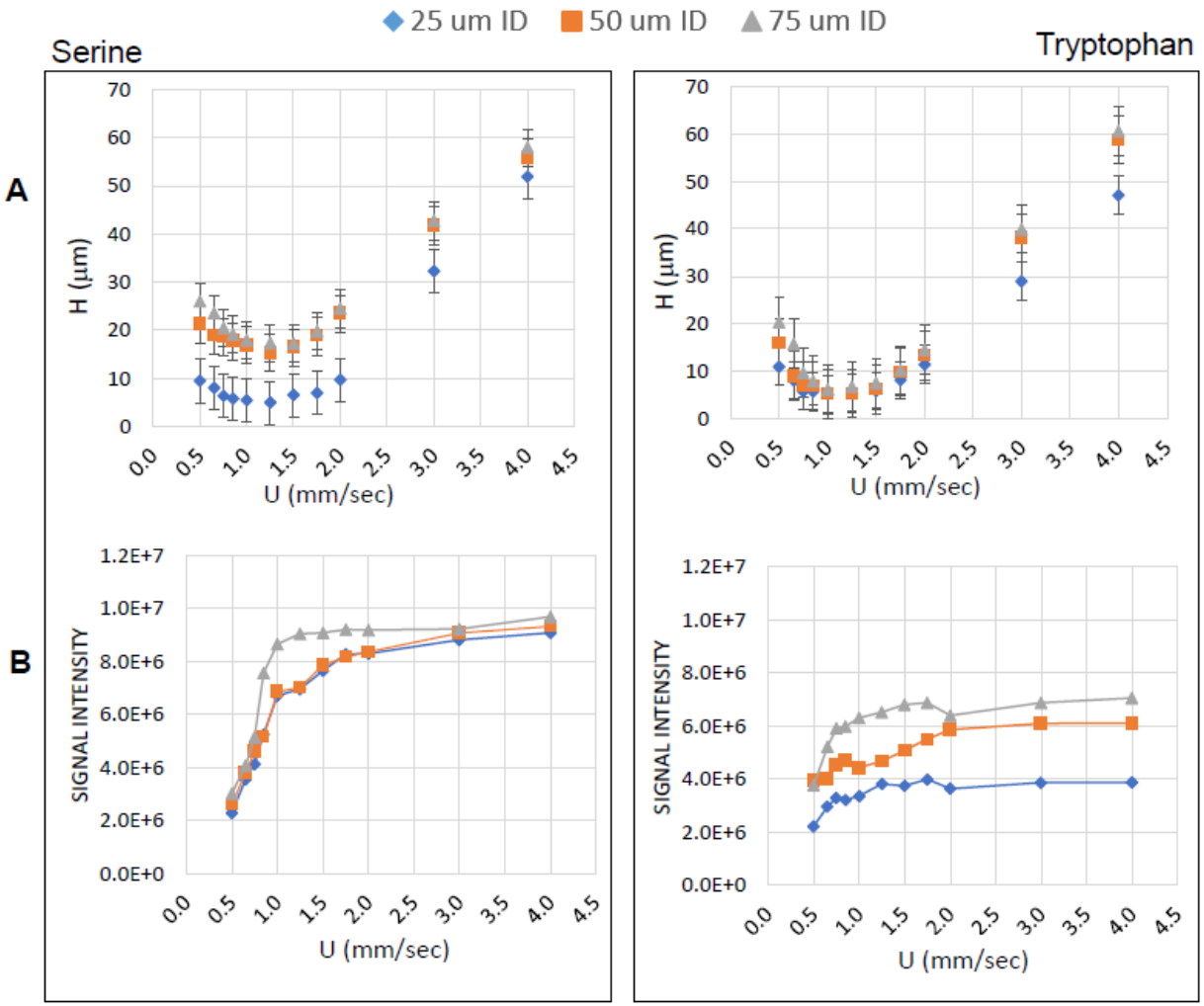

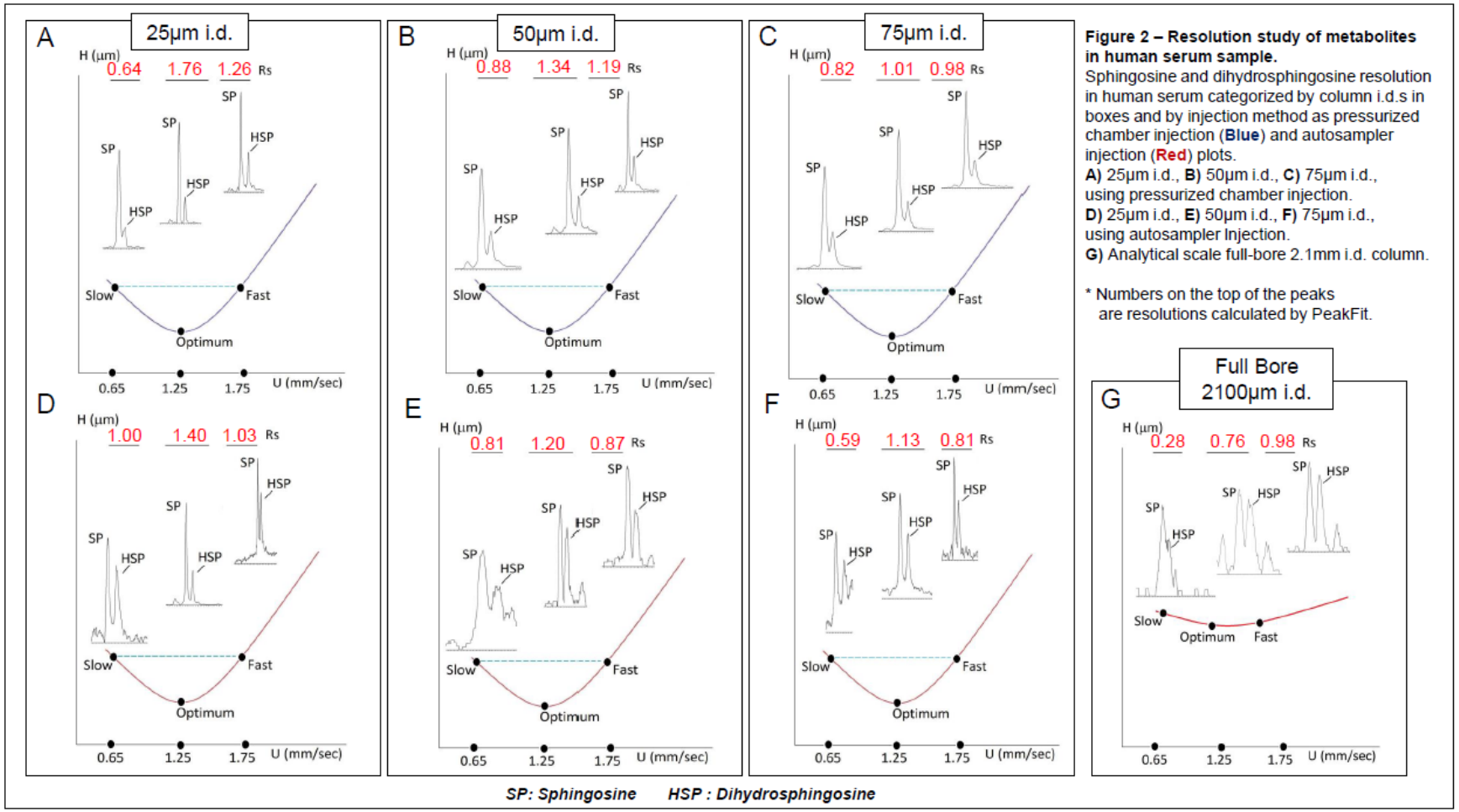

Figure 2 – Resolution study of metabolites in human serum sample.
Sphingosine and dihydrosphingosine resolution in human serum categorized by column i.d.s in boxes and by injection method as pressurized chamber injection (**Blue**) and autosampler injection (**Red**) plots.
A) 25µm i.d., **B)** 50µm i.d., **C)** 75µm i.d., using pressurized chamber injection.
D) 25µm i.d., **E)** 50µm i.d., **F)** 75µm i.d., using autosampler Injection.
G) Analytical scale full-bore 2.1mm i.d. column.

* Numbers on the top of the peaks are resolutions calculated by PeakFit.

Figure 3 – Signal intensity profile of amino acids in human serum and *E. coli* lysate in 2.1mm i.d. full-bore and capillary columns.
Variation of signal intensity of serine, proline, tyrosine, phenylalanine, tryptophan analyzed by nLC-Orbitrap-MS of at the optimized velocity (1.25 mm/sec) in: **A)** Human serum spiked with ^{13}C algal standard and **B)** E. coli lysate. Number on the bars are %RSD (n=3)

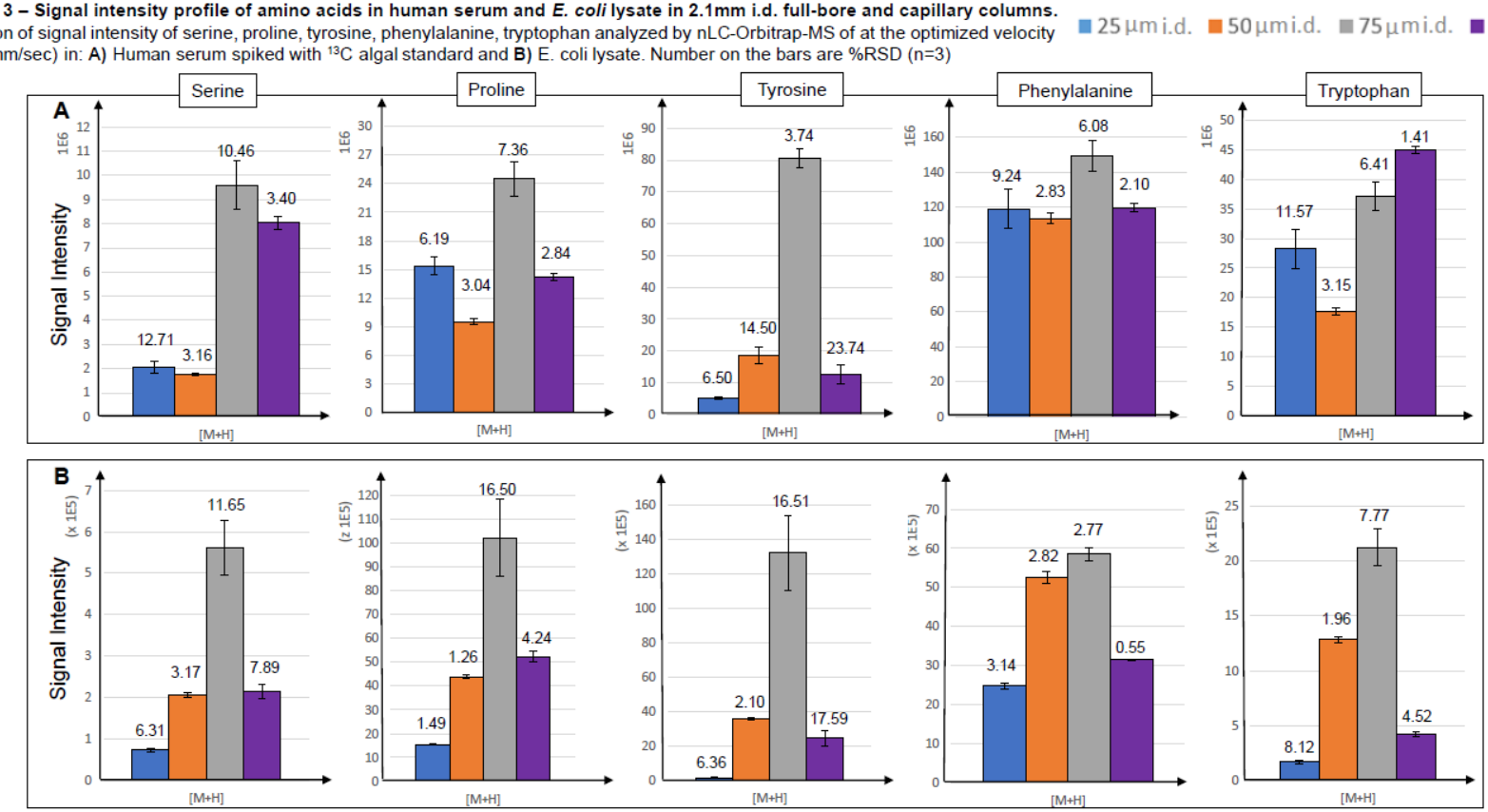

Figure 5 – Degeneracy profile of 2.1mm full-bore and small i.d. capillary columns.
A) Number of degenerate, non-degenerate and total number of features in human serum. **B)** Percentage of annotated, un-annotated, degenerate and total non-degenerate peaks in human serum. **C)** Number of degenerate, non-degenerate and total number of features in *E. coli* lysate. **D)** Percentage of annotated, un-annotated, degenerate and total non-degenerate peaks in *E. coli* lysate.

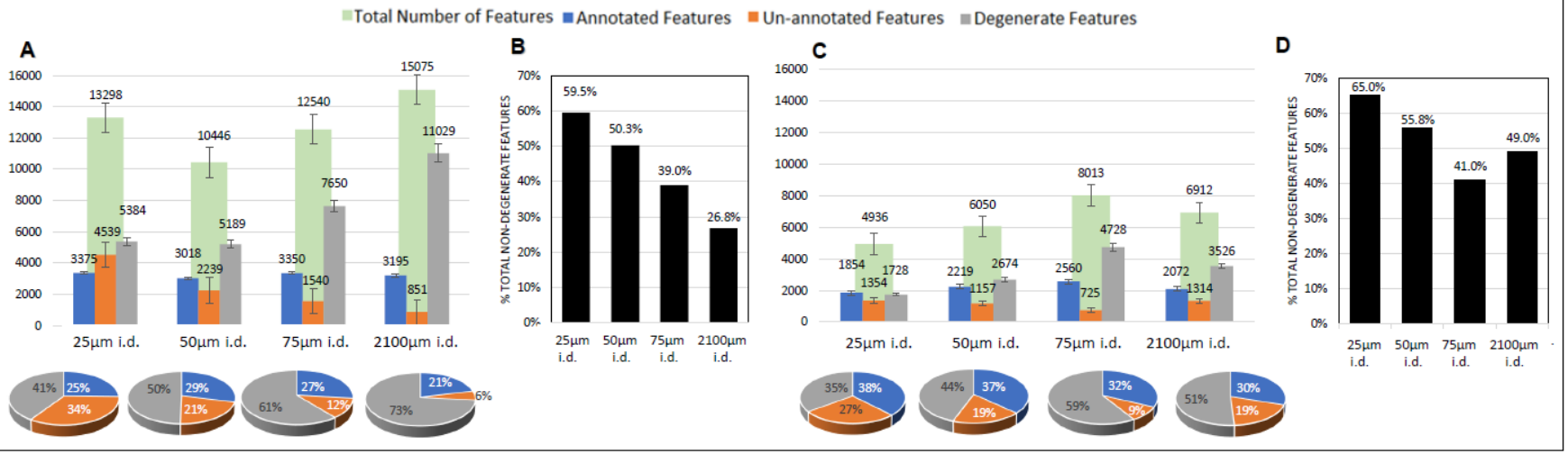

Figure 6 – Comprehensive signal intensity distribution of features in 2.1mm i.d. full-bore and capillary columns in human serum sample.
Signal intensity distribution of all detected features of human serum sample analyzed by XCMS and CAMERA for **A)** 25µm i.d. **B)** 50µm i.d. **C)** 75µm i.d. **D)** 2100µm i.d.
The $[M+H]^+$ and degenerate peaks' intensities of the **E)** Coumaric acid **F)** Kynurenine **G)** N-Acetylphenylalanine **H)** Lauroyl Carnitine annotated features from the highlighted region (signal intensity <1E5) for for 25µm i.d. capillary and 2.1mm i.d. full-bore column.

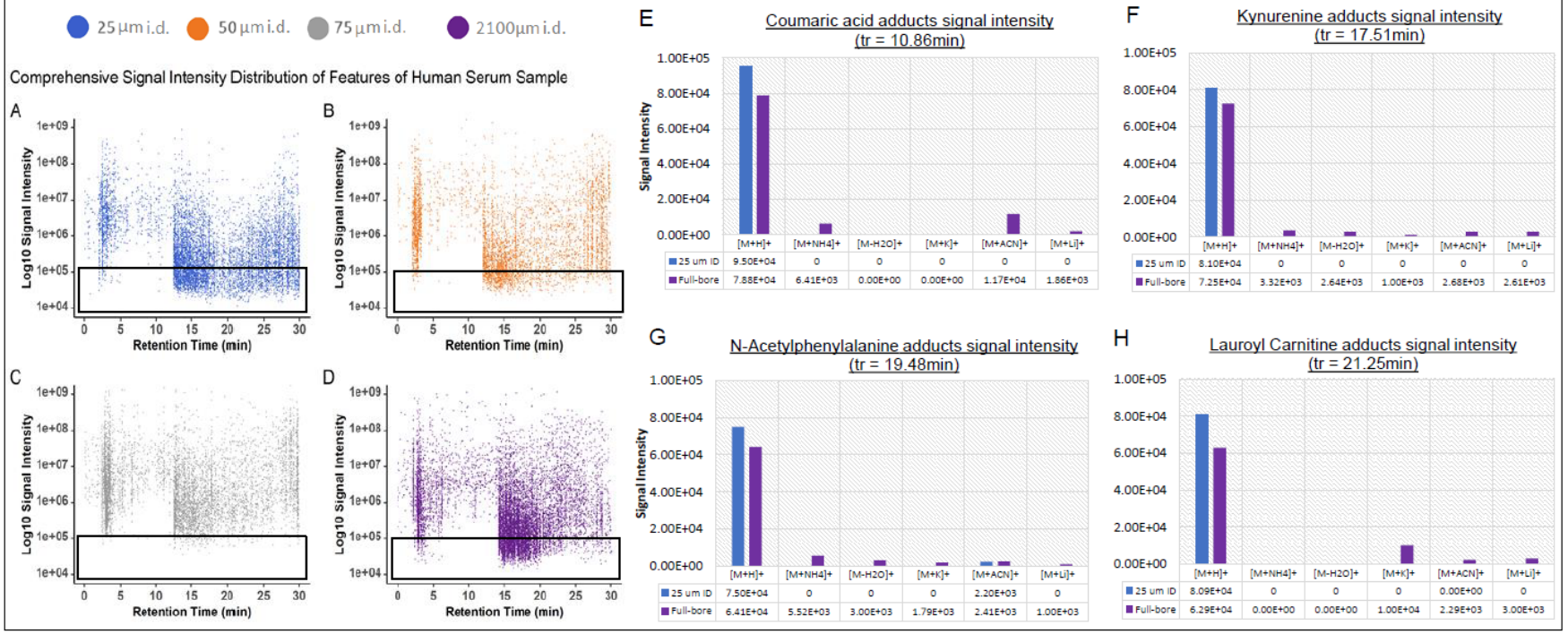

Supplemental Figure S-1 -Variation of HETP of amino acids.
HETP (µm) as a function of linear velocity of Standard amino acids at flow rate from 0.5 to 4.00mm/sec on 25, 50 and 75 µm capillaries and 2100 µm full-bore column of 25µM each of:
A) Serine
B) Proline
C) Tyrosine
D) Phenylalanine
E) Tryptophan

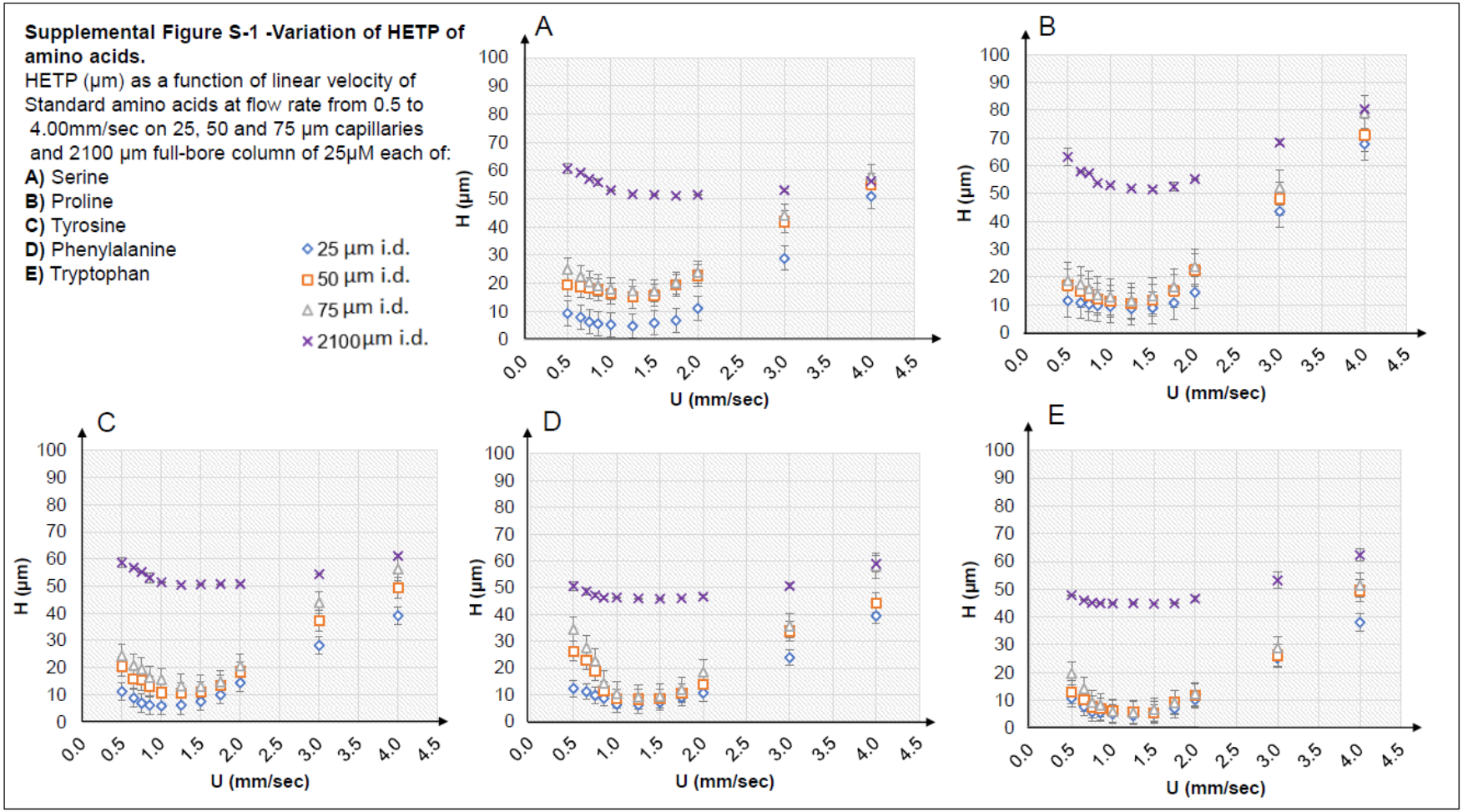

Supplemental Figure S-2 Reduced plate height (h) plots of amino acids.
Variation of reduced plate height a dimensionless measure of the band broadening as a function of reduced velocity (v) for 25µM standard solution of :
A) Serine
B) Proline
C) Tyrosine
D) Phenylalanine
E) Tryptophan

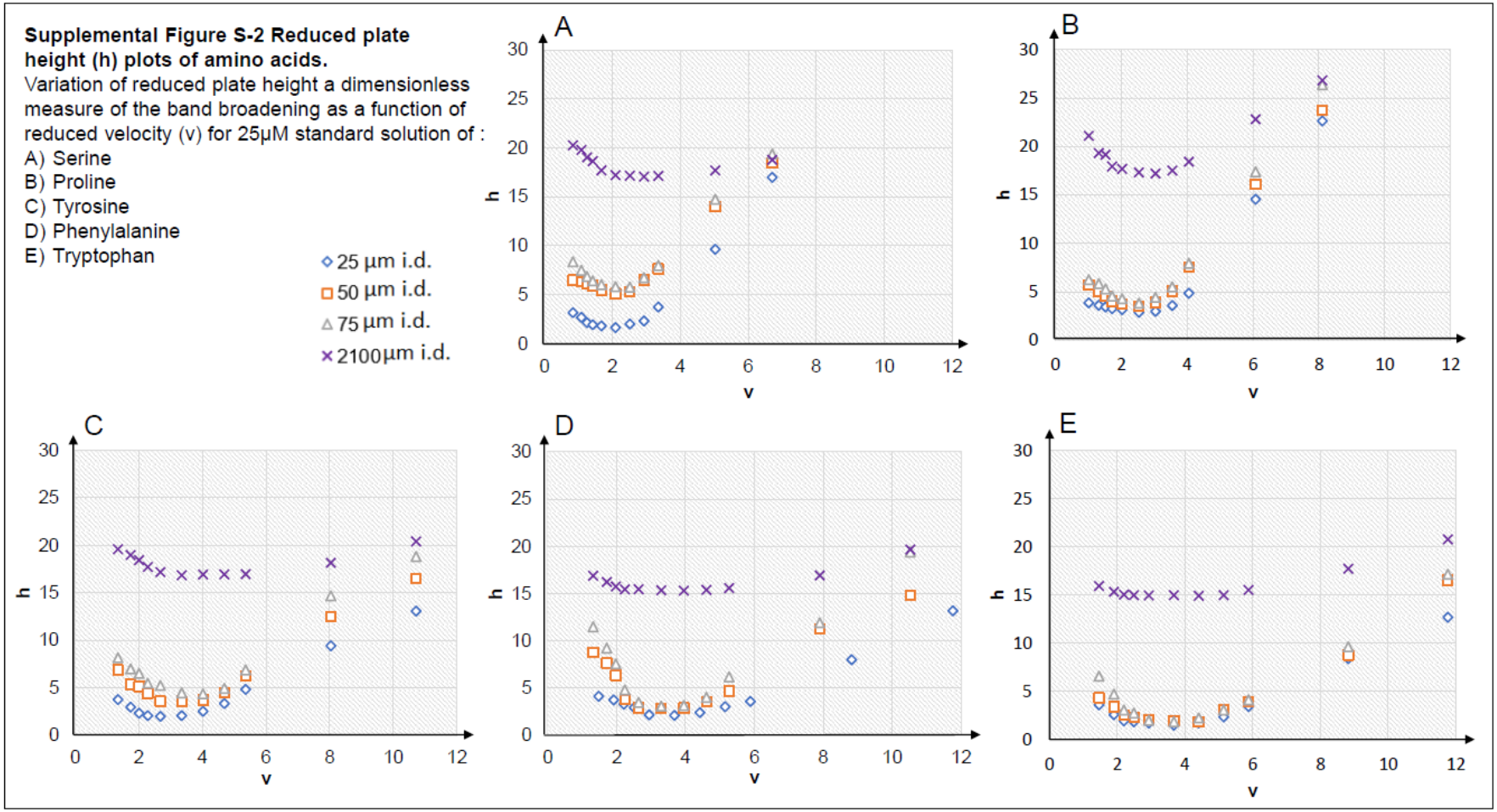

Supplemental Figure S-3 –
Extra column band broadening effect on peak shape.
The peak width w(4σ) trend of serine in suman serum sample infused on the Vanquish-UHPLC-ESI-Orbitrap-MS at different velocities. This was done replacing the 2.1mm column with zero dead volume connection.

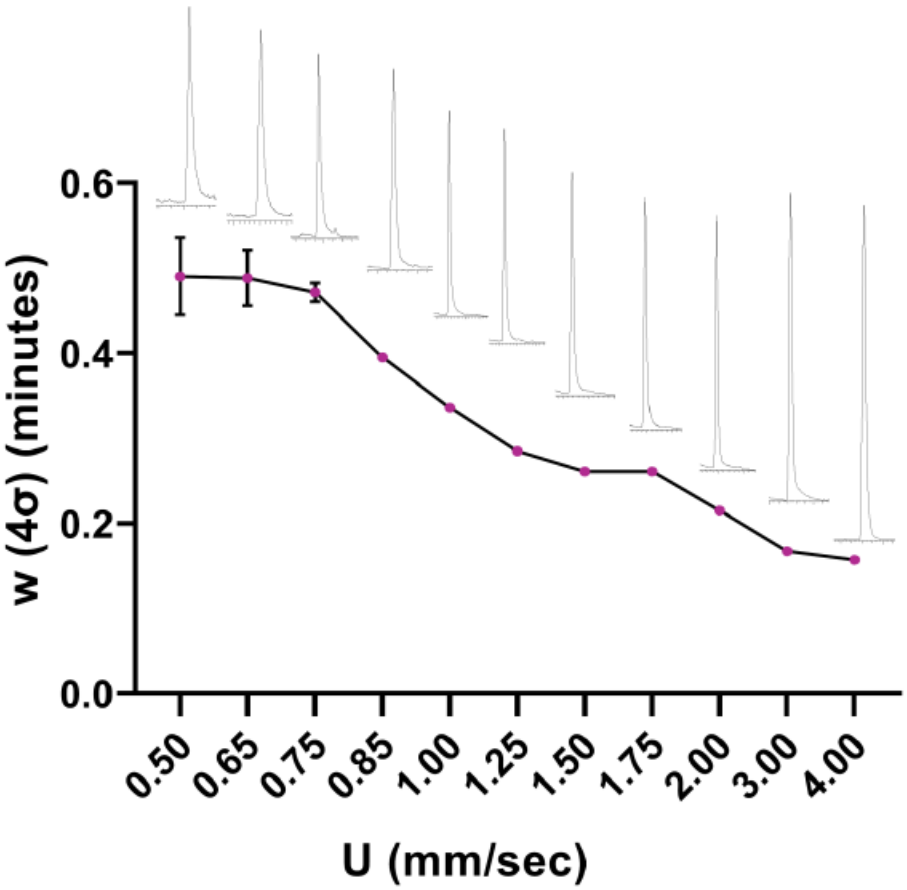

Supplemental Figure S-4 – The shift from mass to concentration sensitive detection over increasing flowrates indicating the difference in nanospray efficiency categorized by capillary column i.d. for:
A) Serine
B) Proline
C) Tyrosine
D) Phenylalanine
E) Tryptophan

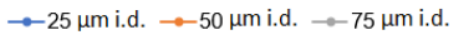

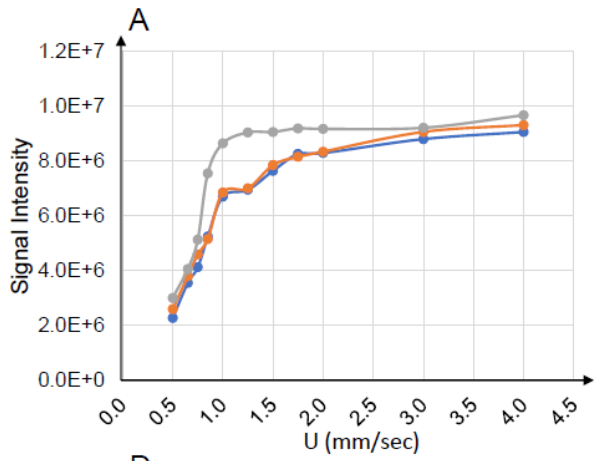

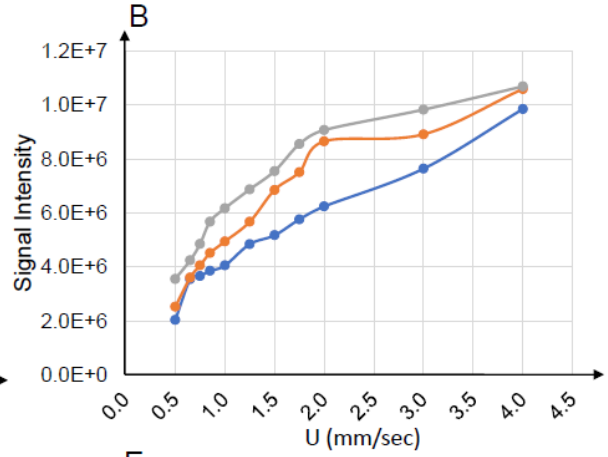

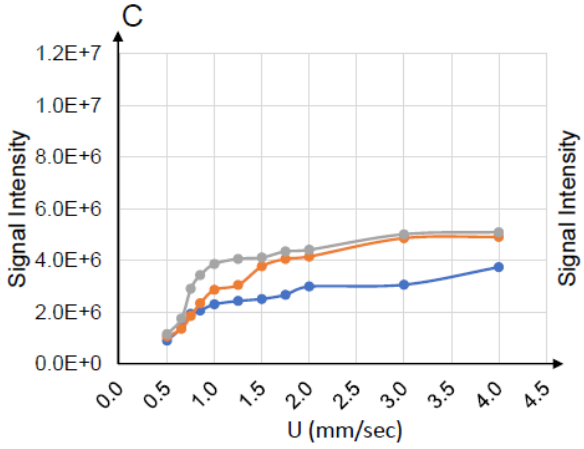

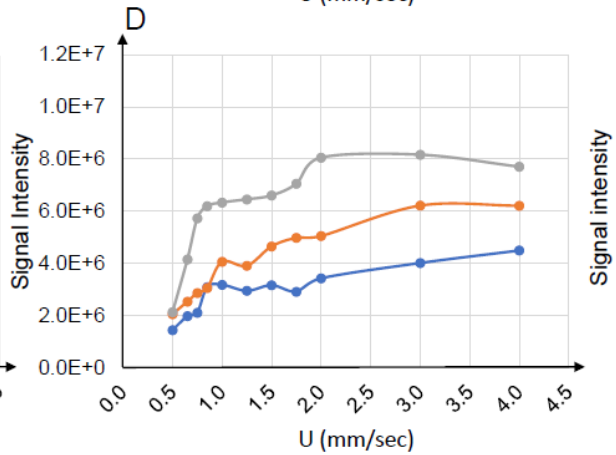

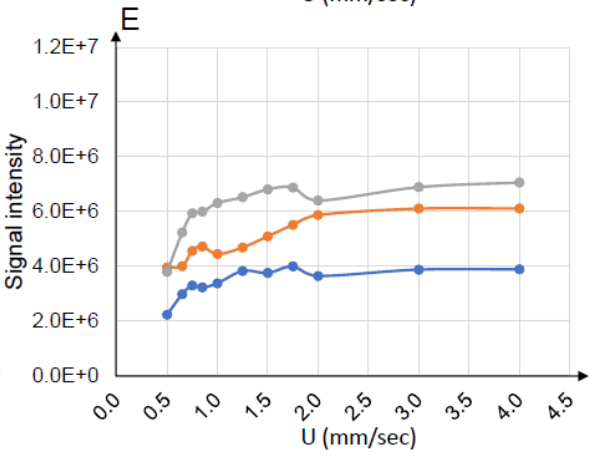

Supplemental Figure S-5 – Fixed mass injection effect on signal intensity.
Injection of a fixed mass on-column of 0.08 nL on the Vanquish-UHPLC-ESI-Orbitrap-MS system using 25, 50, and 75µm i.d. capillaries.
A) Log signal intensity of amino acids standards.
B) Log signal intensity of human serum sample.
C) Signal to noise (S/N) human serum sample.

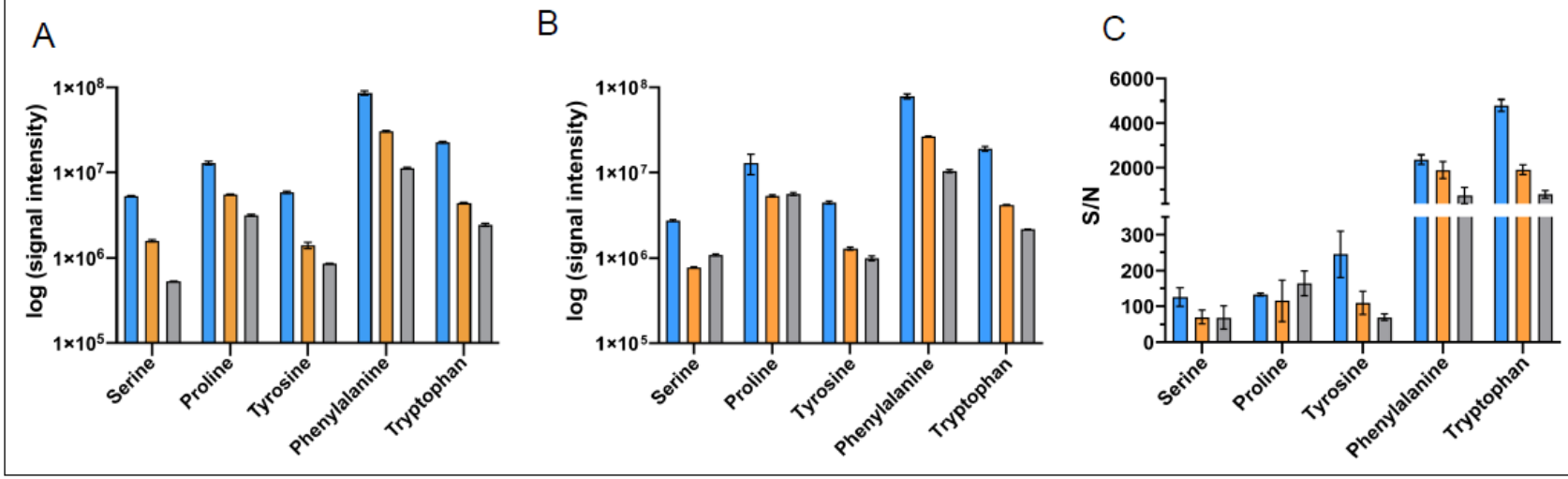

Supplemental Figure S-6 - MSDial fragmentation matches.

Fragmentation patterns of metabolites in data dependent scan of human serum standard sample (Blue) and data base (Red) using MSDial database "All public MS/MS (13,303 unique compounds)" in positive mode having 290,915 record" in a mass tolerance range (0.01 – 0.025).

A) Sphingosine **B)** Dihydrosphingosine **C)** Kynurenine **D)** N-Acetylphenylalanine **E)** Coumaric acid **F)** Lauroyl Carnitine

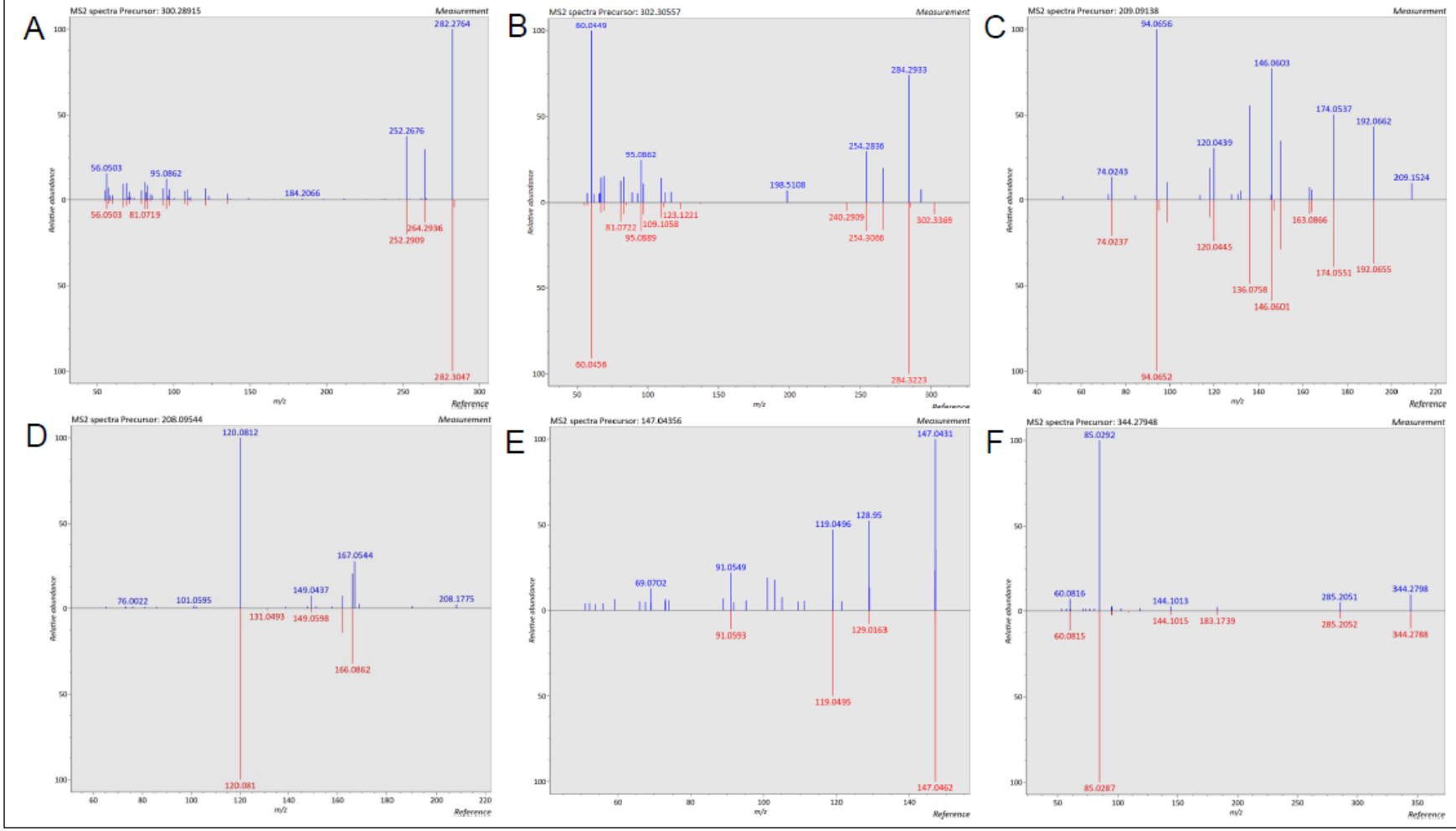

Supplemental Figure S-7 – MS spectrum of proline potassium adducts capillary and full-bore columns.
MS spectrum of proline peaks and its potassium adduct from human serum sample injected in Q-Exactive Orbitrap nLC-MS in **A)** 25 µm **B)** 50 µm **C)** 75 µm i.d. **D)** 2.1mm full-bore column a fixed scale (100x zoomed in for the adducts MS signal 3E4) showing the development of degenerate peak as the column i.d. increase.

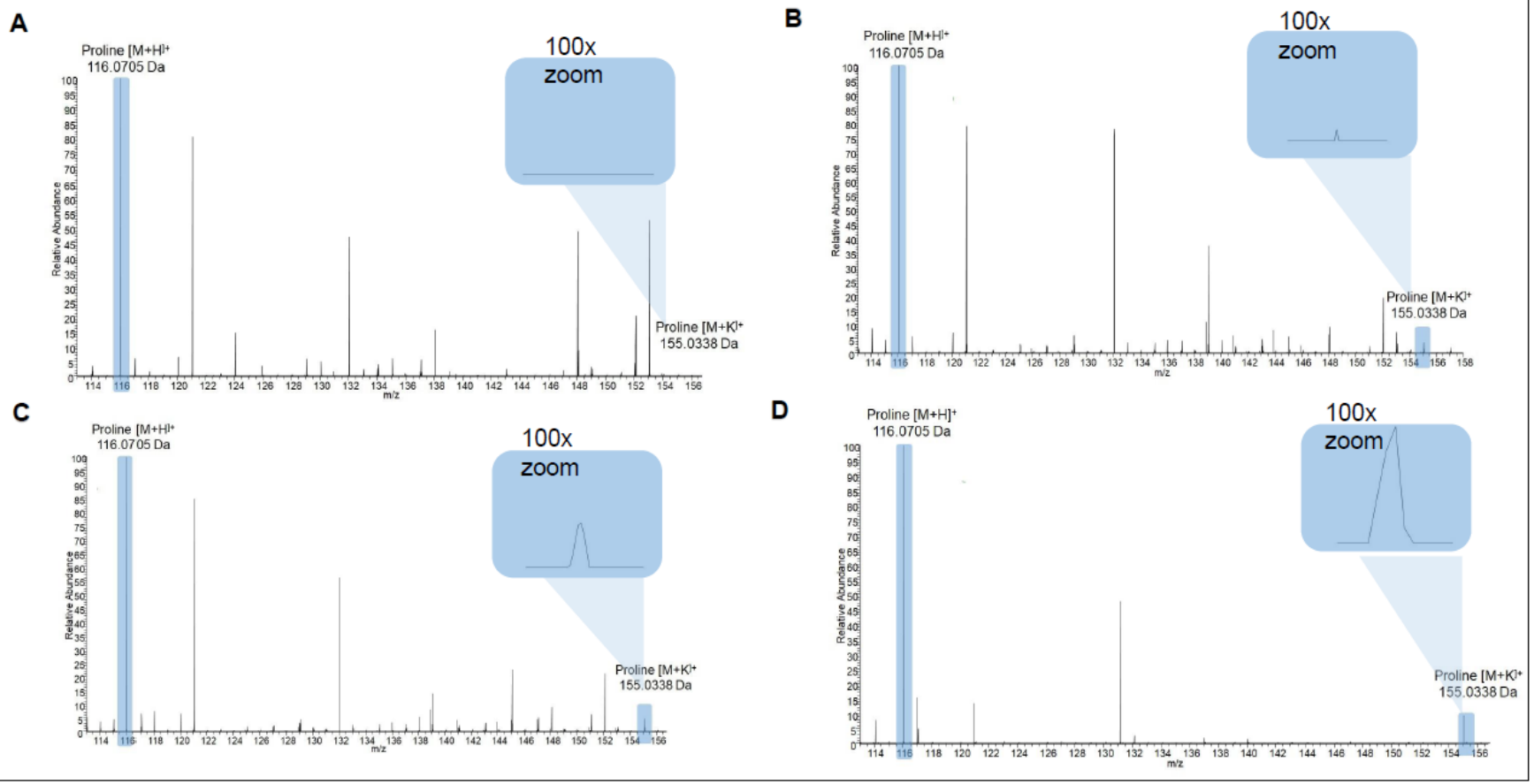

Supplemental Figure S-8 – Venn Diagram of total annotated features in capillary and 2.1mm i.d. analytical scale full-bore column for human serum and *E. coli* lysate

The number of annotated features in **A)** human serum and **B)** *E. coli* lysate showing the common identification across different ESI sources. Data were analyzed by metID and VennDiagram packages. metID package uses HMDB and KEGG database for annotation.

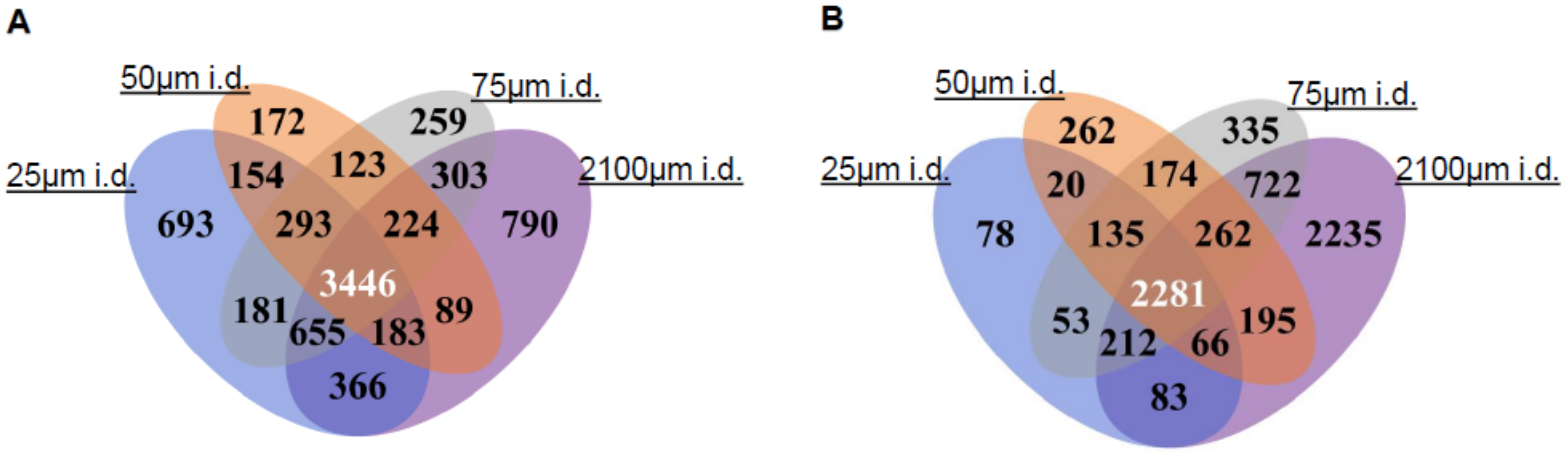

Supplemental Figure S-9 – Comprehensive signal intensity distribution of features in *E. coli* sample.
Signal intensity distribution of all detected features analyzed by XCMS and CAMERA for:
A) 25µm **B)** 50µm **C)** 75µm **D)** 2100µm i.d.

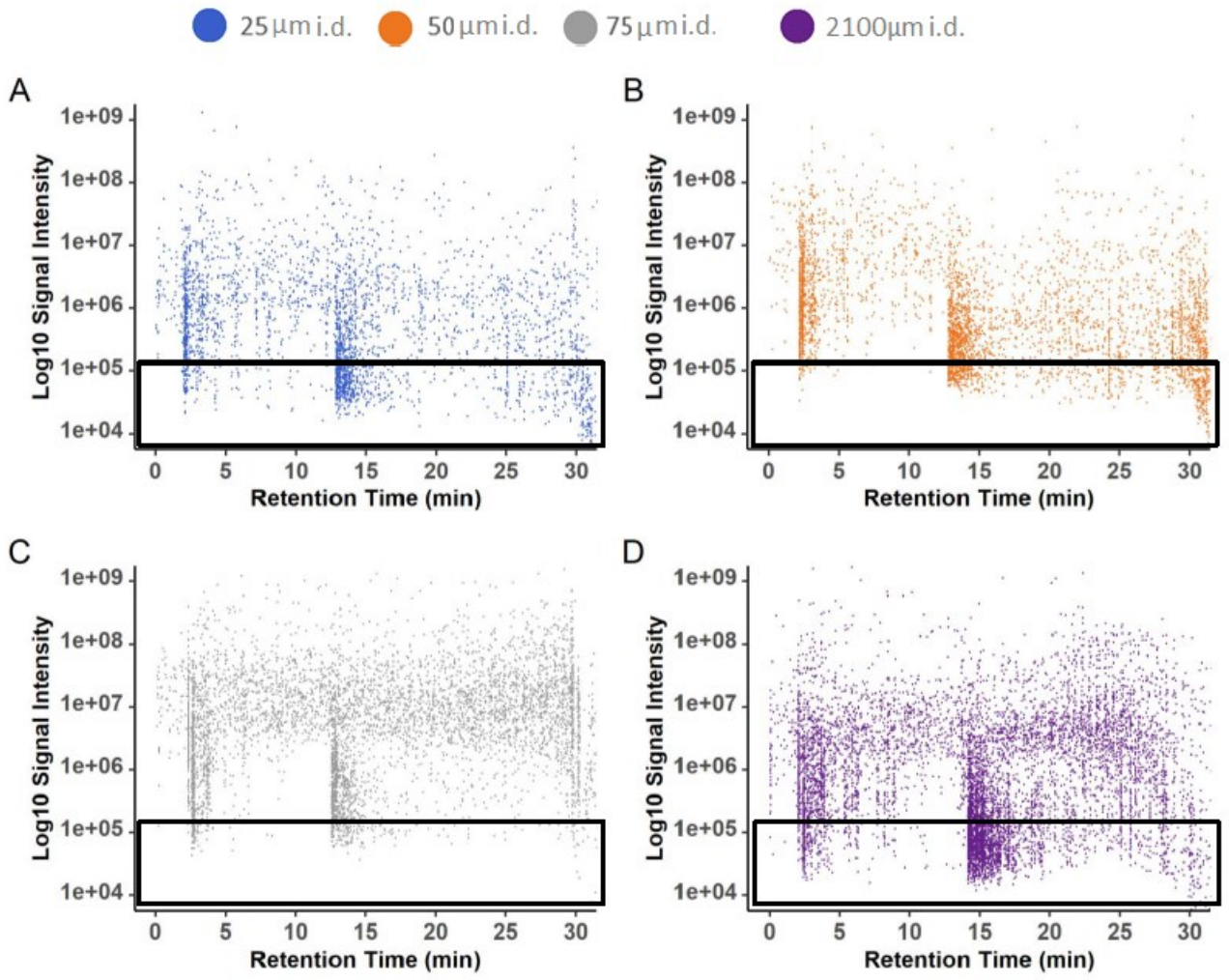

Supplemental Figure S-10 –Total number of degenerate peaks in 25, 50, and 75 µm i.d. capillary and 2.1mm full-bore columns

The number of degenerate peaks of all features throughout the whole chromatogram of the 30 minutes gradient method as each bar represents 1 minutes for **A)** Human serum and **B)** E. *coli* lysate sample.

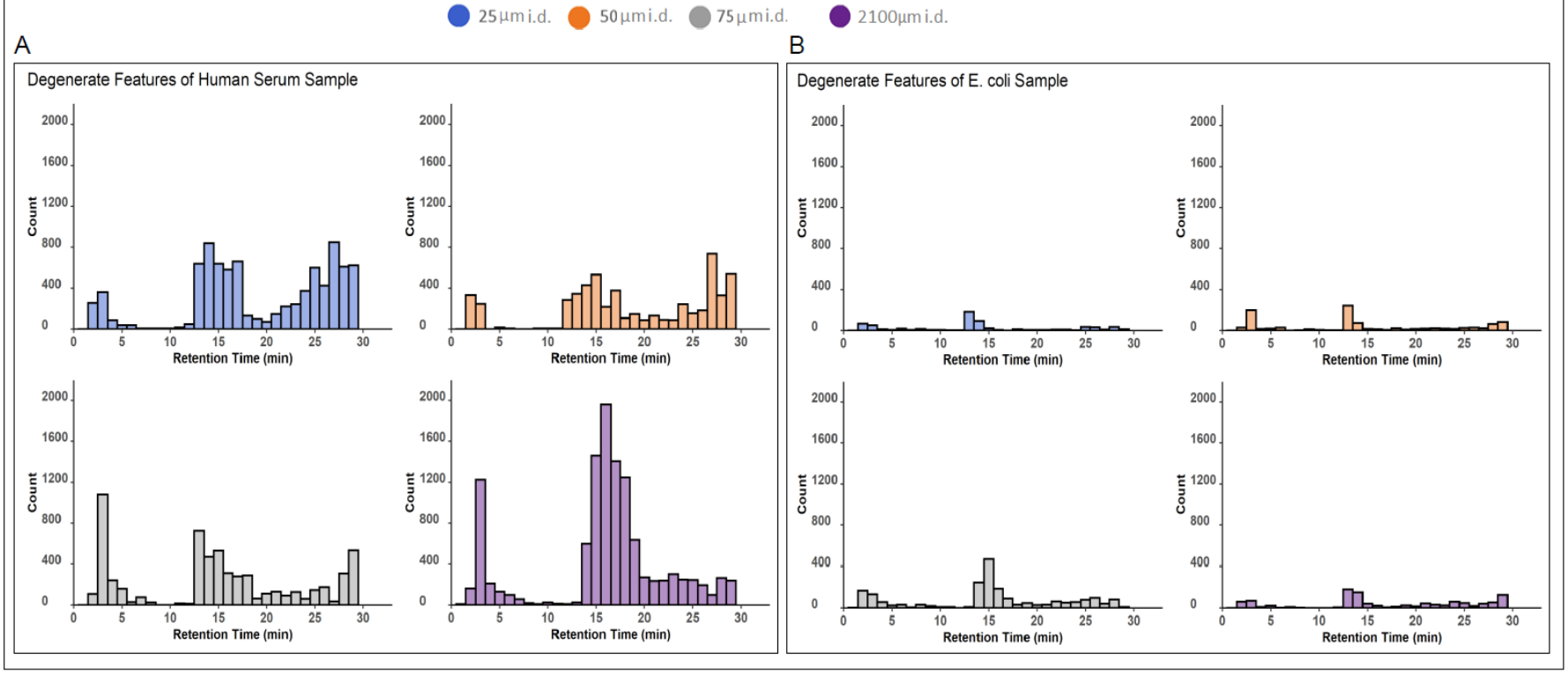

Supplemental Table1: *Tip diameters, averages, and the ratio of i.d.to the tip diameter in (nm) of capillary columns imaged by scanning electron microscope.*

Capillary i.d.	Tip diameter (nm)			Average tip diameter (nm)	Tip/i.d. (µm)
25 µm	428	549	482	486	0.019
50 µm	510	438	685	544	0.011
75 µm	2187	2046	2335	2190	0.029

Supplemental Table2: *(EIC) of MSDial spectrum of serum sample.*
Early, mid, and late eluting identified features in the 30-minutes gradient method.
Peak width at (4σ) 13.4% of maximum signal intensity calculated by PeakFit ®.

t_G	Early eluting analytes			Mid-way eluting analytes			Late eluting analytes		
t_r (min)	5.76	5.90	6.02	12.50	13.71	14.92	20.12	22.24	24.06
Analyte	Citrulline	Arginine	Theophylline	Phenyl Alanine	Indoline	Tryptophan	Climbazol	Sphingosine	Palmitoyl Carnitine
EIC	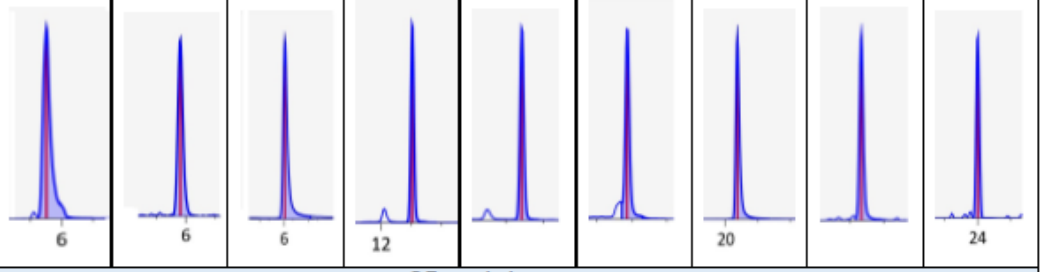								
25µm i.d.									
Trial1	0.32	0.29	0.26	0.23	0.20	0.21	0.17	0.16	0.13
Trial2	0.30	0.28	0.25	0.22	0.19	0.22	0.16	0.15	0.11
Trial3	0.30	0.26	0.25	0.25	0.19	0.20	0.15	0.15	0.10
Avg	0.31	0.28	0.25	0.23	0.19	0.21	0.16	0.15	0.11
Average Peak Width at (4σ) 13.4% above the baseline (min)									0.21
50µm i.d.									
Trial1	0.35	0.30	0.27	0.26	0.25	0.23	0.19	0.18	0.16
Trial2	0.33	0.32	0.24	0.24	0.22	0.22	0.18	0.19	0.17
Trial3	0.32	0.31	0.22	0.22	0.21	0.22	0.16	0.15	0.14
Avg	0.33	0.31	0.24	0.24	0.23	0.22	0.18	0.17	0.16
Average Peak Width at (4σ) 13.4% above the baseline (min)									0.23
75µm i.d.									
Trial1	0.40	0.35	0.32	0.29	0.26	0.27	0.2	0.19	0.15
Trial2	0.37	0.32	0.31	0.28	0.25	0.26	0.19	0.19	0.18
Trial3	0.35	0.30	0.31	0.27	0.25	0.26	0.17	0.17	0.16
Avg	0.37	0.32	0.31	0.28	0.25	0.26	0.19	0.18	0.16
Average Peak Width at (4σ) 13.4% above the baseline (min)									0.26
2100µm i.d.									
Trial1	0.44	0.42	0.37	0.31	0.32	0.3	0.24	0.23	0.22
Trial2	0.42	0.41	0.35	0.30	0.30	0.27	0.22	0.22	0.20
Trial3	0.40	0.39	0.34	0.27	0.28	0.26	0.23	0.22	0.20
Avg	0.42	0.41	0.35	0.29	0.30	0.28	0.23	0.22	0.21
Average Peak Width at (4σ) 13.4% above the baseline (min)									0.30